Redefining Vascular Monitoring: A Wearable with Force Sensor Resistors for Real-Time Pulse Wave Velocity Assessment

Redefining Vascular Monitoring: A Wearable with Force Sensor Resistors for Real-Time Pulse Wave Velocity Assessment

Alessandro Sanginario, *Member, IEEE*, Marco Pogliano, *Member, IEEE*, Irene Buraioli, *Member, IEEE*, Marco Boscherini, *Member, IEEE*, Dario Leone, Alberto Milan and Danilo Demarchi, *Senior Member, IEEE*

***Abstract*— The rising average age in advanced economies is driving an increasingly urgent demand for technological solutions to monitor population health. Given that cardiovascular diseases remain the leading cause of mortality worldwide, the continuous assessment of cardiovascular function has become critically important. In this context, Pulse Wave Velocity (PWV) analysis represents a valuable tool for cardiovascular evaluation. However, the widespread adoption of PWV monitoring remains limited by the absence of wearable devices suitable for continuous use. This work addresses this gap by developing a wearable PWV monitoring device based on Force Sensing Resistor (FSR) technology designed to ensure high wearability. This objective was achieved by creating a miniaturized Printed Circuit Board (PCB) integrating signal acquisition and conditioning circuitry and a Bluetooth Low Energy (BLE) module for wireless data transmission. The data were analyzed by extracting the fiducial point, known as intersect tangent point (ITP), for the estimation of Pulse Transit Time (PTT) and the subsequent calculation of PWV. The system was validated on a cohort of 101 voluntary participants by comparing the PWV values obtained with the proposed device against those measured using the clinical gold standard, SphygmoCor. The results demonstrate a strong correlation between the two measurement systems, with a mean error close to zero ($0.03\,\mathrm{m/s}$) and a standard deviation of ($1.03\,\mathrm{m/s}$). These findings confirm the reliability and accuracy of the proposed solution in a clinical context.**

***Index Terms*— Arterial Stiffness, Bluetooth Low Energy (BLE), Pulse Wave Velocity (PWV), Wearability**

I. Introduction

CARDIOVASCULAR disease (CVD), the leading cause of mortality in the world (17.9 million deaths each year [1]), is a class of disorders involving the heart or blood vessel. Hypertension, affecting approximately 46% of the U.S. population [2], is the major preventable risk factor for CVDs, such as ischaemic heart disease and stroke [3], [4]. The chance of premature mortality due to CVD can be reduced by analyzing several predictive parameters for early disease diagnosis. Among them, arterial stiffness is a key prognostic index and potential therapeutic target in hypertensive subjects for its close relation to the vessels' elastic characteristics [5], [6]. Indeed, a high arterial stiffness reduces the ability of the vessels to control blood flow and overloads the heart, bringing it to cardiac hypertrophy [7]–[9].

In this scenario, monitoring vascular stiffness is of increasing clinical relevance. Nowadays, the most widely used method to clinically assess this parameter consists of the measurement of Pulse Wave Velocity (PWV), which corresponds to the velocity employed by the blood pressure pulse to circulate through the cardiovascular system. It represents the primary way to assess arterial rigidity non-invasively. The two are directly linked: the stiffer the vessel walls, the faster the pulse wave [10]. The standard method for evaluating PWV is the carotid-femoral acquisition (cf-PWV) [11]. This involves acquiring signals from two anatomical sites: the carotid artery in the neck and the femoral artery, which is superficially located halfway between the symphysis pubis and the anterior superior iliac spine. Specifically, the velocity is obtained by the ratio between the distance d that separates them (which is multiplied by a corrective factor of 0.8 to approximate the actual pathway) and the Pulse Transit Time (PTT) [11]. This corresponds to the time the pulse travels between the two acquisition sites. For this, the final velocity is calculated as in Equation 1:

$$PWV = \frac{0.8 * distance}{PTT}. \tag{1}$$

PWV measurement can be performed using two distinct approaches, commonly called the two-step and one-step methodologies. The two-step method relies on the electrocardiographic (ECG) signal as a temporal reference to realign pulse waveforms acquired at two different anatomical sites in a non-simultaneous manner. Specifically, the peak of the QRS complex is used as a reference point to calculate the propagation delay of the pulse wave at the carotid and femoral arteries relative to the ECG. The transit time is then obtained by computing these two delays' differences. In contrast, the one-step method involves the simultaneous acquisition of the

Alessandro Sanginario, Marco Pogliano, Irene Buraioli, Marco Boscherini, and Danilo Demarchi are with the Department of Electronics and Telecommunications, Politecnico di Torino, 10129 Torino, Italy (e-mail: alessandro.sanginario@polito.it; marco.pogliano@polito.it; irene.buraioli@polito.it; marco.boscherini@polito.it; danilo.demarchi@polito.it).

Dario Leone and Alberto Milan are with the Candiolo Cancer Institute FPO-IRCCS, Division of Internal Medicine, Department of Medical Science - University of Turin, 10060 Candiolo (TO), Italy (e-mail: dario.leone@ircc.it; alberto.milan@ircc.it).

TABLE I: Main clinical commercial devices for Pulse Wave Velocity assessment.

DEVICE	SENSOR	EXECUTION MODE	COST	WIRELESS	WEARABILITY
SphygmoCor Vx	Tonometric	Two step	•••••	-	-
SphygmoCor XCEL	Tonometric	One step	•••••	-	-
Pulse Pen	Tonometric	Two step	•••	-	-
Vicorder	Cuff-based oscillometry	One step	••••	-	-
Arteriograph	Cuff-based oscillometry	One step	•••••	-	-
Complior	Piezoelectric	One step	•••	-	-
Our system	FSR	One step	••	✓	✓

two pulse waveforms, allowing for a direct calculation of the time difference between the signals without requiring the ECG as a reference. Over the years, various transduction technologies have been proposed for assessing cf-PWV. Applanation tonometry is the most widely used approach (SphygmoCor Vx [12], [13], SphygmoCor XCEL [14], [15], Athos [16], PulsePen [17]). Piezoelectric mechanotransducer (Complior [18]), cuff-based oscillometry (Vicorder [19], Arteriograph [20]), and photoplethysmography (MPPT [21]) are the other methods used for non-invasive arterial stiffness measurements. Ultrasound technique and MRI remain confined to clinical research [22]. In recent years, smartwatches and smart rings, based on photoplethysmographic technology, have begun to revolutionize the field of physiological monitoring in sports and wellness applications. Although these tools are still far from achieving clinical validation for the estimation of cf-PWV, they undoubtedly represent a promising technological advancement. Table I presents a comparative analysis of the main characteristics of devices currently used in clinical settings for cf-PWV measurement. Specifically, the table compares the type of sensor employed, the acquisition methodology, the indicative cost, the data transmission modality, and the level of wearability. Each of these parameters plays a critical role in enabling the use of PWV measurement as a large-scale cardiovascular risk screening tool [23], particularly in non-specialist settings.

In this context, commercial devices for clinical PWV estimation present some criticisms. They are expensive, making them difficult to be used on a large scale in supra- and outpatient facilities for repetitive monitoring of such vital parameters. In addition, they require considerable operator expertise, which could profoundly affect the measurement. As demonstrated in [24], the two main sources of variability in the measurement of cf-PWV are the method used to determine the distance and the operator's level of training, both of which significantly affect the accuracy of the test. These factors also represent a potential limitation to the use of PWV only in highly specialized hospital settings. The requirement for the presence of trained healthcare personnel makes none of the currently available clinical devices suitable for long-term monitoring aimed at tracking the temporal evolution of PWV, even in ambulatory or low-trained structures. For these reasons, the widespread clinical adoption of PWV measurement remains limited to date [25]. Force Sensing Resistor (FSR) have been investigated to overcome these limitations. FSRs are part of the most prominent force sensor family, including strain gauge, piezoelectric, and piezoresistive sensors. In strain gauges, resistance variation is related to conductor deformation since the electrical resistance of conduction is a function of its mechanical dimensions. Piezoelectric sensors generate an electric charge when subjected to mechanical stress, a phenomenon known as the piezoelectric effect. However, parasitic capacitances and leakage currents often affect the generated charge, requiring complex front-end circuitry for accurate voltage measurement. Instead, the piezoresistive effect is based on the conductivity variation due to an external force. These sensors are easily constructed utilizing flexible materials, are very resistant to noise, have simple conditioning electronics, are inexpensive, and have a small sensing area. All these features make them ideal for designing an innovative wearable device. Flexible pressure sensors based on materials such as reduced graphene oxide [26] have also been investigated, although FSRs offer a particularly advantageous balance of cost, mechanical resilience, and ease of use for wearable biomedical devices.

The proposed study, based on previous considerations, validates an innovative wireless system for PWV measurement on a cohort of 101 voluntary subjects, using SphymoCor Vx as reference. The system is based on the use of a FSR for the acquisition of the pulse waveform and is designed to overcome several practical and clinical limitations of current PWV measurement technologies. Specifically: (a) it enables one-step PWV assessment without the need for ECG signals, thereby simplifying the acquisition workflow; (b) sensor positioning requires minimal operator training and is facilitated by elastic bands for initial placement; (c) the use of flexible and robust FSRs ensures reliable skin contact and effective pulse wave detection in a wearable format; (d) the integrated graphical user interface (GUI) provides real-time visualization of both carotid and femoral signals, supporting clinicians during data acquisition; (e) the overall system architecture and component selection are cost-effective, promoting scalability and facilitating large-scale clinical deployment.

The document is structured as follows: Chapter II provides an overview of the system; Chapter III details the circuit implementation and explores aspects related to the wearability of the proposed solution; Chapter IV examines the signal processing techniques used for physiological parameter extraction; Chapter V presents the measurement protocol; Chapter VI presents a critical analysis of the results obtained from experimental

acquisitions; Chapter VII outlines the conclusions drawn from the work conducted.

II. System Overview

The present work aims to extend the application of PWV measurement to a broad range of clinical contexts by developing a portable, wearable, low-cost device. The outcome is a compact and user-friendly solution capable of ensuring high standards of accuracy and reliability. As in Fig. 1, the system comprises three main components: the hardware for signal acquisition and transmission, the receiving unit, and the patented PWV analysis and estimation algorithm [27].

The system employs a low-cost commercially available force sensing resistors, positioned at the carotid and femoral arteries, to acquire pulse wave signals used for estimating PTT. The detected signals are then processed by Analog Front-End (AFE) circuits mounted on dedicated PCBs, which filter and amplify the signals before digitization, carried out by an integrated 12-bit Analog-to-Digital Converter (ADC). A System-on-Chip (SoC) with integrated Bluetooth Low Energy (BLE) functionality manages wireless data transmission to a computer. A custom firmware for the SoC has been developed, carefully designed to avoid data loss during transmission with an optimized data transmission rate for visualization and further processing. A dedicated Graphical User Interface (GUI) enables user interaction and supports visualization and analysis of the pulse waves in real time. The pulse waveform signal was sampled at 1 kHz to obtain a sufficiently detailed temporal resolution, enabling precise detection of the rising edge associated with the systolic peak, which typically occurs over a timespan of only a few milliseconds. Additionally, the software provides options for saving data, enabling further analysis using external tools. To synchronize carotid and femoral pulse wave acquisitions, we employed a purely hardware-based scheme. The two acquisition boards are hardwired via dedicated GPIO lines; on each microcontroller, one line is configured as an output and the other as an input. The interconnect uses spring-loaded contacts (see Fig. 2a). At initialization, both outputs are driven low, while the inputs are armed to generate an interrupt on a rising edge. When the user initiates recording from the graphical interface, pull-up resistors on the link lines produce the low-to-high transition, causing both microcontrollers to begin sampling in lockstep. This direct wired coupling keeps relative clock drift negligible over the short acquisition windows used here (on the order of minutes), thereby preserving signal synchrony without any changes to the BLE stack. Signal analysis and PWV estimation are handled by a dedicated post-processing algorithm, as detailed in Section IV. A compact rechargeable lithium battery powers the system, maintaining a portable and space-efficient form factor, making it well-suited for dynamic clinical environments.

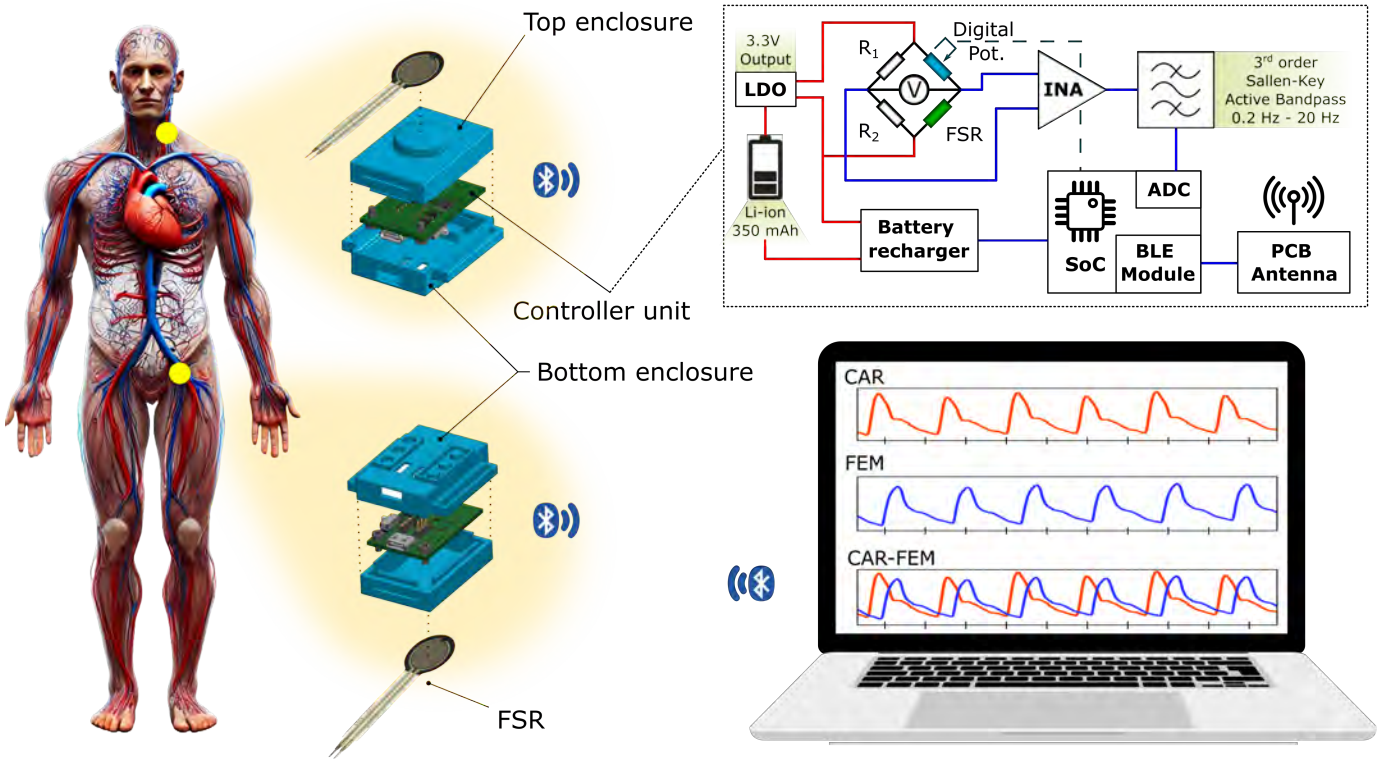

Fig. 1: The proposed system consists of two Analog Front-End (AFE) modules, each integrating a Force Sensing Resistor (FSR), signal acquisition and conditioning electronics, and a wireless data transmission unit. Communication is established via Bluetooth Low Energy (BLE) protocol to a dedicated dongle, which forwards the acquired signals to a laptop. A real-time Graphical User Interface (GUI) is executed on the laptop, enabling the pulse waves visualization and analysis.

III. Circuit Implementation

The circuit implementation of the wireless PWV measurement device was a critical aspect of this work, focused on achieving signal integrity, low power consumption, and compactness. This chapter details the design and assembly of the hardware, including the sensor interface, signal conditioning circuits, and the wireless communication system. The main goal was to create a reliable, low-cost system while maintaining the accuracy and portability required for wearable biomedical devices.

A. Sensor Interface and Conditioning Circuit

The FSR convert pulse-induced pressure variations into resistance changes, which are then processed to reconstruct the vascular waveform. This pressure deforms two layers of printed, flexible piezoresistive ink, resulting in a proportional change in electrical resistance. Such variation can be measured using a dedicated circuit that converts the resistance change into a voltage signal suitable for sampling and digital analysis [28]. Due to their mechanical flexibility and environmental robustness, FSRs are well-suited for this application, enabling stable contact with the skin and accurate detection of pulse-induced displacement [29] at arterial sites. Following an analysis of commercially available FSR components and a comparison of their main technical characteristics, including size, sensitivity, and operating range, the FSR 402 model (Interlink Electronics, USA) was selected as the most suitable option for this application, given the dynamic nature of the pulse wave signal to be captured. The sensor features a force sensitivity in the range $0.2\,\mathrm{N}$ to $10\,\mathrm{N}$, a force repeatability of $\pm 2\%$, and has been tested for durability up to 10 million actuations. The sensor was selected to operate in shunt mode, in respect to thru mode, due to its superior performance in this specific application, as demonstrated by C. Lebossé et al. in previous comparative studies of shunt- and thru-mode FSR configurations [30], [31]. In FSR design, shunt-mode devices route current laterally through a top FSR-ink layer into interdigitated electrodes when pressure brings the conductive layers into contact, whereas thru-mode devices place the FSR ink and conductive silver on opposite sides of the spacer in a mirrored PET-encapsulated stack, so pressure drives current vertically through the layer pair.

Each sensor is positioned at anatomically significant locations, notably over the carotid and femoral arteries, where the pulse wave signal is most prominent. The signal conditioning circuit plays a critical role in amplifying the weak signals originating from the sensors and in suppressing unwanted disturbances, such as motion artifacts and environmental interference, thereby improving signal fidelity. The circuit architecture consists of three primary components arranged sequentially: a Wheatstone bridge, an instrumentation amplifier, and a series of filtering stages. The Wheatstone bridge provides a simple yet robust solution for precisely detecting small resistance changes. In this implementation, it integrates the FSR sensor along with a digital potentiometer. The potentiometer dynamically balances the bridge by adjusting its resistance according to the baseline pressure applied to the sensor. This baseline value is strongly influenced by sensor placement conditions and the tension of the securing strap. The adjustment of the digital potentiometer is controlled via firmware, as detailed in the following section. The output signal from the bridge is then directed to an instrumentation amplifier, which ensures high common-mode rejection and amplifies the signal to a level suitable for subsequent digitization. This stage is essential to maintain the signal amplitude within an optimal range, thereby avoiding saturation or distortion. To eliminate high-frequency noise and slow baseline drift, the circuit incorporates a third-order Sallen-Key low-pass filter and a corresponding high-pass filter. These selective filters allow only physiologically relevant frequency components of the pulse wave signal to pass, typically ranging between $0.2\,\mathrm{Hz}$ and $20\,\mathrm{Hz}$. The signal is then transferred to the ADC integrated within the SoC responsible for data transmission. The ADC converts the continuous analog signal into digital format, making it suitable for wireless transmission and real-time processing.

B. System Control and Wireless Communication

The robustness of the proposed system with respect to sensor placement is ensured through an initial calibration phase, during which the value of the digital potentiometer embedded in the Wheatstone bridge is optimized. This adjustment maximizes the quality of the output signal by adapting it to the variations in force detected by the sensor and, consequently, to the measured electrical resistance. At system startup, the potentiometer is initially set to a predefined value, selected based on average adaptability considerations. Subsequently, via SPI interface, the potentiometer is recalibrated based on the mean of the data acquired during the first five seconds of recording. This process compensates for any offset pressure introduced by the specific placement of the sensor on the subject. The system's control and wireless communication capabilities are pivotal for real-time data transmission without the need for cables. The system employs BLE technology, selected for its low power consumption, high data transmission rates, and suitability for wearable applications. The BLE module is implemented using an STM32WB55 SoC, integrating both the BLE transceiver and the processing core. This module transmits the digitized pulse wave data acquired from the sensors to an external laptop. To maintain continuous and real-time communication, the digitized pulse wave data is packaged into BLE data packets and transmitted at regular intervals. Each BLE packet contains 16 interleaved 16-bit samples (8 per channel), resulting in a payload of 32 bytes per packet. At a sampling rate of 1 kHz per channel, the system transmits approximately 125 BLE packets per second, totaling 4 kB/s. This data rate is well within the capabilities of the BLE 5.0 protocol, ensuring reliable and lossless real-time communication. No modifications were made to the standard BLE stack as implemented on the STM32WB55 platform. To enhance robustness, the system leverages a high sampling frequency that naturally mitigates the impact of occasional packet loss. Moreover, the PTT estimation algorithm [16] is robust by design and tolerant to sporadic missing samples, ensuring stable performance even in non-ideal transmission conditions.

(a) Wearable enclosures (45x42x20)mm (b) System in hospital

Fig. 2: (a) Wearable enclosures housing the internal PCBs. (b) System applied to a test subject during clinical testing.

C. Power Consumption

The device is powered by a compact 3.7 V rechargeable lithium-ion battery, selected for its high energy density and recharging capability. This battery connects to a power management circuit comprising a charger IC and a low-dropout (LDO) linear voltage regulator. The charging circuit facilitates recharging via a standard USB connection, while the LDO regulator ensures a stable 3 V supply to the SoC and other components. To optimize energy efficiency, the SoC employs power-saving modes during idle periods, thereby reducing overall consumption. In [32], a study conducted by the same research group was presented, which uses a completely different sensor setup but adopts a Bluetooth transmission protocol similar to the one used in this study. The work observed that energy consumption was almost exclusively due to data transmission, while signal acquisition and conditioning contributed negligibly. Therefore, it is reasonable to refer to the previously validated results to estimate the energy consumption and battery life of the new device. The average current consumption is estimated to be approximately $6\,\mathrm{mA}$; considering a battery with a capacity of $350\,\mathrm{mAh}$, the system is capable of ensuring a full day of use in a hospital environment without the need to recharge. This current estimation specifically refers to the active BLE transmission phase, during which the device continuously streams data at the configured sampling rate, with the ADC resolution, data format, and BLE protocol exactly matching those used in real operating conditions. No additional transmission overhead was introduced, as the native communication protocol inherently alternates packets from the carotid and femoral sensors in sequence.

D. Wearability and ease of use

The integration of the wireless PWV measurement system into a wearable form factor was a key focus of this work, ensuring portability, user comfort, and accurate data acquisition in both clinical and potential point-of-care solutions. The system was designed to be compact, lightweight, and non-intrusive, allowing users to wear the device without discomfort. None of the participants reported experiencing any discomfort or skin irritation during the study. A housing for the two integrated PCBs was designed and 3D printed (Fig. 2a), featuring flanges that allow an elastic band to pass through, enabling the system to adapt to any body size and shape (Fig. 2b). The FSR extends out of the housing and, through a controlled bending, is securely adhered to a raised bump on the backside wall of the casing. This configuration minimizes signal path lengths, resulting in reduced noise, enhanced compactness, and improved management. The two units of the device interlock using a mechanism similar to Lego bricks; thus, connecting the USB-C cable to one unit charges both simultaneously. This is achieved through spring-loaded connectors that, when the two parts are joined, establish electrical contact for both power transfer and the hardware-level synchronization of the acquisition boards.

IV. Signal Processing

This section examines the signal processing procedure applied to the carotid and femoral recordings acquired using the proposed device during experimental trials. The analysis workflow consists of two main phases: an initial signal pre-processing stage, followed by the extraction of fiducial points required for estimating the temporal delay and, subsequently, computing the PWV. A hybrid approach combining key elements from the algorithms described in [16] and [33] was developed and tailored to optimize the processing of the signals collected with the proposed system.

A. Pre-processing

The acquired data were sampled at $1\,\mathrm{kHz}$ frequency to ensure a high representativeness of the pulse wave morphology. From each recording, the final 12 seconds are extracted, excluding the last 2 seconds in order to obtain a 10-second segment for analysis. This time window was chosen to make the data comparable to those processed by the clinical gold standard. The truncation is justified by the fact that, during the examination, the clinician monitors the signal quality in real-time and ends the acquisition when they deem the trace sufficiently stable and free from artifacts, allowing for

a reliable estimation of the physiological parameter. The last two seconds are excluded as they may be subject to motion artifacts, often induced by the operator's interaction during the final phase of acquisition. The selected data undergo a digital filtering operation to remove any out-of-band components. For this purpose, a fourth-order Butterworth low-pass filter with a cutoff frequency of $10\,\mathrm{Hz}$ is applied, followed by a fifth-order high-pass filter with a cutoff frequency of $0.5\,\mathrm{Hz}$. The visual inspection performed by the clinicians was complemented by a quantitative assessment of signal quality, based on the calculation of the average signal-to-noise ratio (SNR) across all acquisitions. The results showed an average SNR of approximately 18.8 dB for the carotid signals and 17.8 dB for the femoral signals, confirming the high quality of the recorded waveforms and the reliability of the proposed system in capturing the pulse wave.

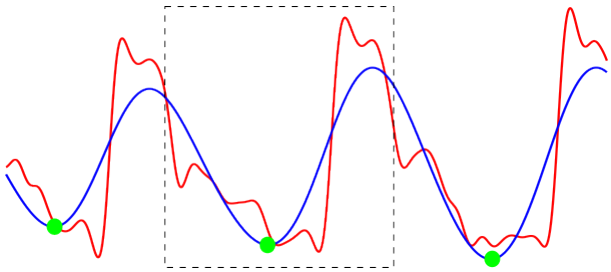

(a) Minimums (green) of $1.5\,\mathrm{Hz}$ low-pass filtered (blue) original signal (red)

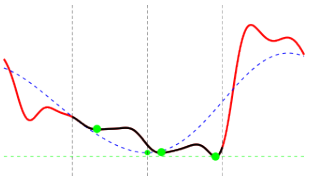

(b) Foot Wave Identification (green)

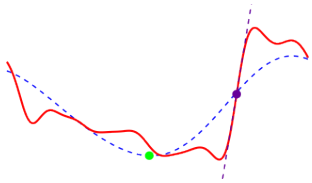

(c) Maximum Derivate Tangent (purple)

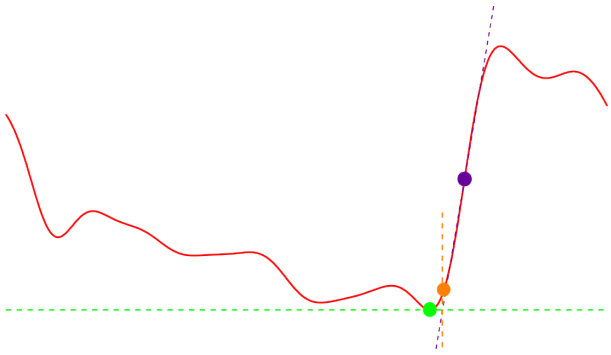

(d) Intersect Tangent Point Identification (orange)

Fig. 3: Algorithm for the intersect tangent point identification, as (a) minimum of the $1.5\,\mathrm{Hz}$ low-pass filtered signal; (b) Foot wave identification; (c) Maximum derivative tangent; (d) Intersect Tangent Point as projection of the intersection between foot wave horizontal line and maximum derivative tangent. Time and amplitude scales are intentionally omitted, as they depend respectively on the subject's heart rate and sensor placement/pressure.

B. Fiducial Point and PWV evaluation

Various algorithms have been proposed for estimating the time delay between signals, including the intersecting tangent point (ITP) method, and approaches based on the second derivative [34]. Among these, the intersecting tangent point method is the most commonly implemented in clinical devices, owing to its robustness across a wide range of operating conditions. The previous filtered signal is then analyzed to identify the ITP for calculating the temporal phase shift between pulse waves. With reference to the representative example signal shown in Fig. 3, to facilitate detection, zero-padding is applied at both the beginning and end. The minima are then identified by applying a low-pass filter with a cutoff frequency of $1.5\,\mathrm{Hz}$ (Fig. 3a). With this process, the oscillatory pattern associated with the pulse waves is isolated, providing a robust initial reference even in the presence of noise. The minima identified on the filtered signal are used as starting points to search for the foot wave as defined in [16] (Fig. 3b). Once the foot wave is located, the maximum of the derivative of the signal is calculated within the neighborhood, and the parameters of the tangent line at this point are determined, (Fig. 3c). The projection on the curve of the intersection between this tangent line and the horizontal line passing through the minimum, allows for the identification of the so-called intersect tangent point (Fig. 3d). This procedure is applied to both the carotid and femoral acquired signals. A comparative analysis of the extracted points is then performed, pairing them correspondingly for each cardiac wave. At this stage, all ITPs without a corresponding counterpart in the other signal acquisition site are discarded. Additionally, pairs that produce a temporal delay significantly divergent from the observed mean behavior, outside the range mean $\pm$ 1.5 times the standard deviation, are also excluded. The pairs of points that meet all quality criteria are used to calculate the average temporal delay between the two signals. Finally, applying Equation 1, the value of the PWV is estimated.

V. Measurement Protocol

Following the design and technical development of the proposed system, a clinical validation phase was conducted in collaboration with the medical team of the "A.O.U. Città della Salute e della Scienza di Torino", with clinical experience in PWV measurement protocols. A total of 101 volunteer subjects participated in the study. The trial was approved by the ethics committee of the University of Turin (UniTO), and all participants provided informed consent for the use of their data for research purposes.

To assess the performance of the developed device, the SphygmoCor system was adopted as the clinical gold standard for PWV estimation. The evaluation protocol was designed to ensure comparability between the two systems under controlled and reproducible conditions.

The population was selected in accordance with the recommendations presented in [35], specifically for the comparison between devices for estimating PWV, to ensure good heterogeneity among the subjects. The inclusion criteria required participants with no prior history of cardiovascular disease or

conditions that could influence arterial stiffness. The exclusion criteria comprised a Body Mass Index (BMI) $> 40\ \mathrm{kg\,m^{-2}}$; age < 18 or > 82 years; a history of stroke, diabetes, or hypertension; pregnancy; or any significant medical condition that could alter cardiovascular function. The reference parameters for these variables are age (17 subjects < 30, 14 subjects 30–49, 58 subjects 50–69, and 12 subjects ≥ 70 years), gender (55 women vs. 46 men), height ($166\,\mathrm{cm} \pm 10\,\mathrm{cm}$), weight ($69.2\,\mathrm{kg} \pm 13.8\,\mathrm{kg}$), PWV range measurements (11 subjects ≤ 6 m/s, 12 subjects with ≥ 10 m/s, and 42 subjects with ≥ 8 m/s).

The sensors were positioned over the carotid and femoral arteries using elastic bands, as illustrated in Fig. 2b. This configuration makes the system quick to wear and limits operator involvement mainly to the initial correct placement of the sensors. Since the positioning procedure may introduce differences in band tension and, consequently, in the baseline level applied to the sensors, a calibration step is performed immediately after placement in order to compensate for this effect before starting the acquisition. Once calibration is completed, the pulse waves are recorded and the PWV is subsequently calculated according to Equation 1. The measurement of PWV requires, in addition to signal acquisition, the determination of the distance between the two measurement sites.

As is commonly done in clinical practice, the distance was measured using a flexible tape measure with a resolution of 1 mm. The three key distances required by the protocol were recorded: the distance from the carotid site to the sternum, the distance from the femoral site to the sternum, and the direct distance between the two measurement sites. These measurements are typically performed together to ensure the correct identification of signal acquisition points and to guarantee consistency in the collected data.

Each subject underwent three acquisition sessions using both devices, with an average duration of a few minutes per acquisition. Within each session, both the device and the medical operator were alternated, replacing the device each time. This device alternation was implemented to minimize the temporal gap between the measurements, as simultaneous data acquisition was impossible. Similarly, alternating medical operators, maintained consistently in consecutive subjects, was intended to reduce potential bias arising from operator-specific skills. As shown in Fig. 4, Operator A, who performed the SphygmoCor acquisition on subject *i*, subsequently conducted the developed device acquisition on subject *i+1*.

VI. Measurement Results

A. Outliers Analysis

For each device, three independent measurements were conducted to ensure the procedure's repeatability and provide statistical significance to the results. The three values obtained for each device on each subject were evaluated individually to assess their reliability. If any of the three values deviated by more than 15% from the median of the corresponding triplet, it was excluded from further analysis, as it was considered to be affected by a measurement error unrelated to the monitored physiological parameter. This exclusion criterion is commonly adopted in clinical settings for this type of measurement to preserve the robustness and reliability of the physiological data. The inter-subject variability observed across the measurements still demonstrated good agreement between the two devices, with the average standard deviation over the three acquisitions being substantially comparable. Due to clinical constraints, it was impossible to acquire data synchronously, and thus, a direct comparison of paired values between the two devices could not be performed. Instead, the PWV values for each subject were averaged, yielding a single representative value per device.

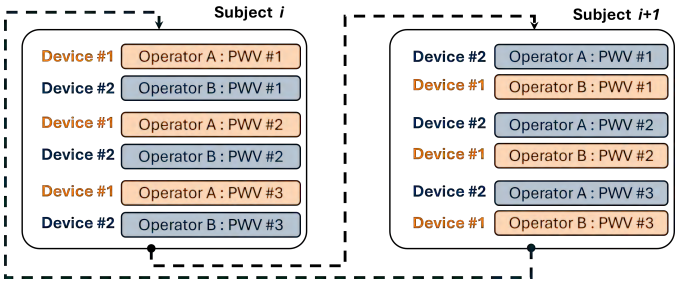

Fig. 4: The acquisition protocol involving the proposed device and SphygmoCor was designed to eliminate operator bias and minimize the time interval between measurements, thereby ensuring uniform and comparable experimental conditions.

B. Performance validation and discussion

Performance evaluation was carried out through a paired comparison between PWV values obtained using the developed device and those provided by the clinical gold standard, SphygmoCor. Fig. 5a displays the correlation plot between the measurements acquired from the two devices, with a color-coding scheme representing the age of the subjects to whom the data refer. A strong correlation between chronological age and PWV values is immediately apparent, a well-documented phenomenon in the literature, highlighting the progressive increase of this physiological parameter with advancing age. Furthermore, a high degree of agreement is observed between the data collected by the two devices, supporting the validity of the proposed system. To numerically assess the correlation between the measurements, Pearson coefficient (0.823), Spearman coefficient (0.809), Lin's coefficient (0.823) and Interclass Correlation Coefficient (0.824) were calculated. All values exceed 0.8, which is commonly used in the literature as the threshold to define a strong linear correlation.

The Bland-Altman graph, which illustrates the agreement between results acquired from two different devices, is reported in Fig. 5b. The bias between the two measurements is negligible, amounting to $+0.03\,\mathrm{m/s}$, demonstrating that the proposed device does not introduce any systematic shift in the measurement of the physiological parameter, with a standard deviation of $1.03\,\mathrm{m/s}$. The upper and lower limits ($\pm 2\sigma$) in the plot correspond to $2.09\,\mathrm{m/s}$ and $-2.03\,\mathrm{m/s}$, respectively.

In [35], the reference values are provided for defining a new device relative to the gold standard, specifically for PWV.

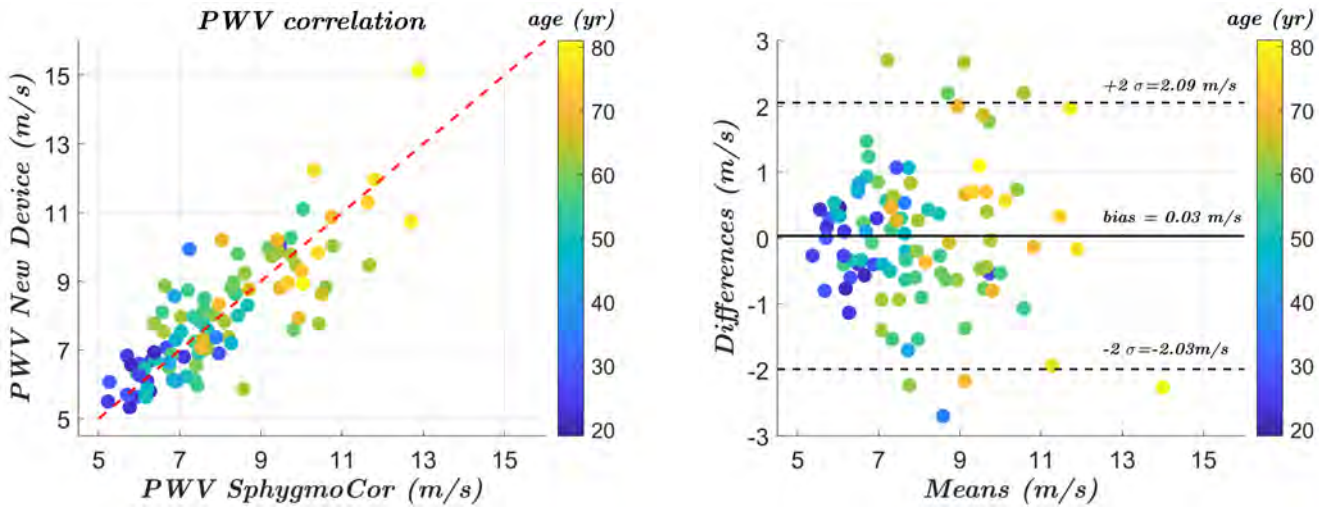

(a) Correlation graph (b) Bland-Altman graph

Fig. 5: (a) The scatter plot shows a linear correlation between the values acquired by the two instruments across all subjects and further highlights the well-established correlation between PWV values and age; (b) Bland-Altman plot that compares the performance of the suggested system and those offered by SphygmoCor.

For each mean bias value on the Bland-Altman plot, the standard deviation value is reported to define good accuracy and acceptable accuracy. In this case, these values correspond to $0.694\,\mathrm{m/s}$ and $1.042\,\mathrm{m/s}$. These two thresholds ensure that 85% of the measurements have an error lower than 1 m/s, which is a clinical reference value to guarantee accuracy and reliability. Therefore, with the obtained values, it is demonstrable how the proposed device's performance is consistent with the gold standard for PWV estimation. To further deepen the analysis, we performed an age-stratified error assessment based on the four classes defined by clinical recommendations. The results show a mean error ($\pm$ standard deviation) of $0\,19 \pm 0.56\,\mathrm{m/s}$ for subjects aged < 30 years, $0\,01 \pm 1.04\,\mathrm{m/s}$ for the 30–49 years group, $0\,09 \pm 1.11\,\mathrm{m/s}$ for the 50–69 years group, and $0\,03 \pm 1.03\,\mathrm{m/s}$ for subjects aged 70 years. These preliminary results suggest that the mean error remains broadly stable across the different age groups, whereas the error variability tends to increase with age, as reflected by the higher standard deviations observed in the older strata. Despite this increase in dispersion, overall performance remains consistent with ranges that are commonly considered acceptable in clinical practice. It should be noted, however, that these estimates have limited statistical strength, as they are derived from small subsamples of the dataset. Consequently, this analysis will need to be confirmed on larger and more balanced cohorts, and it will represent a key element of the planned future work. To assess measurement repeatability, we computed the mean of the within-subject standard deviations across triplicate measurements. The resulting values, $0.40\,\mathrm{m/s}$ for SphygmoCor and $0.63\,\mathrm{m/s}$ for the proposed device, indicate that, while the prototype exhibits slightly higher variability, its performance remains consistent across repeated acquisitions.

Across the cohort of 101 participants, the device demonstrated high accuracy once the sensor was correctly positioned at the measurement site. When benchmarked against the clinical gold standard and evaluated within current medical directives, the system met the required criteria for clinical reliability. Measurement stability was also likewise comparable to the reference device. Residual discrepancies are plausibly explained by protocol constraints, most notably the impossibility of perfectly synchronized and co-located acquisitions. The two systems cannot be operated concurrently and consequently, physiological variability, including short interval fluctuations in heart rate, may alter PWV estimates and contribute to small discrepancies.

C. Limitations and Future works

We acknowledge three main limitations that should be addressed to further strengthen the generalizability of the validation: population restrictions, measurement constraints, and the limited scope for subgroup (group-wise) stratification. These design choices were aligned with current validation recommendations and are appropriate for a first-stage clinical assessment. Nevertheless, broader population coverage, more controlled comparative measurements, and deeper subgroup analyses would improve external validity. Future work will therefore focus on expanding the dataset to enable finer-grained stratified analyses and to reinforce generalization, including a systematic evaluation of pathological cohorts to quantify performance in patients with overt cardiovascular disease. We also plan to extend the system toward ambulatory and home-care scenarios by rigorously assessing robustness to motion artifacts against established clinical devices, and by defining practical artifact-management strategies. These will include automated detection of severely corrupted acquisitions and protocol-level repetition when needed. In addition, we will investigate multi-element FSR sensor matrices to reduce sensitivity to operator-dependent placement and to relax positioning requirements. To further strengthen the robustness of

the analyses, future studies should also include a multi-device comparative evaluation, in order to assess performance not only against SphygmoCor, but also in comparison with other devices already validated in clinical practice. Such an approach would also enable a more accurate and comprehensive assessment of the measurement error, helping to better disentangle device-specific effects from the intrinsic limitations of the proposed system.

On the technology side, future improvements will include further device miniaturization, the integration of additional sensors to broaden physiological monitoring, and validation within larger clinical trials. In parallel, we also plan to evaluate alternative sensing solutions, including smaller sensor designs, in order to improve wearability and facilitate integration into a more compact system. For multi-hour monitoring, we will incorporate protocol-level time synchronization within the BLE stack, leveraging established approaches to ensure robust long-term signal alignment under wireless operation [36], [37]. Collectively, these developments will consolidate the device's potential as a practical solution for both clinical deployment and personal health monitoring.

VII. Conclusions

This work successfully demonstrated the development and optimization of a wireless, wearable system for the measurement of PWV, a crucial parameter for assessing arterial stiffness and cardiovascular health. The system integrates FSR sensors, signal conditioning circuits, and BLE technology to create a compact and portable device capable of real-time, non-invasive monitoring. One of the primary objectives of this project was to eliminate the use of cables and enhance the portability of traditional PWV measurement systems. By incorporating BLE for wireless data transmission and a compact, rechargeable lithium-ion battery, the device achieves autonomy and ease of use, making it suitable for supervised clinical assessments and promising for future everyday/home applications, pending dedicated usability testing and real-world validation. The device was designed to provide accurate, reliable data while maintaining low power consumption and ensuring user comfort. The custom firmware ensures efficient data transmission and real-time monitoring, while the GUI offers an intuitive platform for viewing and analyzing the collected data. The validation was performed by experienced clinicians on a cohort of 101 volunteer subjects. The comparison with the gold standard device demonstrated a high reliability of the proposed solution, adhering to the recommendations provided by the medical-scientific community for the validation of a new device. The system's portability and ease of use make it a promising tool for widespread cardiovascular monitoring, potentially enabling earlier detection of arterial stiffness and improved management of cardiovascular diseases.

References

[1] A. Timmis, D. Kazakiewicz, N. Townsend, R. Huculeci, V. Aboyans, and P. Vardas, "Global epidemiology of acute coronary syndromes," *Nature Reviews Cardiology*, pp. 1–11, 2023.

[2] J. M. Giacona, W. Kositanurit, J. Wang, U. B. Petric, G. Khan, D. Pittman, J. W. Williamson, S. A. Smith, and W. Vongpatanasin, "Utility of standing office blood pressure in detecting hypertension in healthy adults," *Scientific Reports*, vol. 13, no. 1, p. 15572, 2023.

[3] D. Kingsmore, B. Edgar, M. Rostron, C. Delles, and A. Brady, "A novel index for measuring the impact of devices on hypertension," *Scientific Reports*, vol. 13, no. 1, p. 13651, 2023.

[4] F. D. Fuchs and P. K. Whelton, "High Blood Pressure and Cardiovascular Disease," *Hypertension*, vol. 75, no. 2, pp. 285–292, 2020.

[5] H. Fok and J. K. Cruickshank, "Future Treatment of Hypertension: Shifting the Focus from Blood Pressure Lowering to Arterial Stiffness Modulation?" *Current hypertension reports*, vol. 17, pp. 1–8, 2015.

[6] M. E. Safar, "Arterial stiffness as a risk factor for clinical hypertension," *Nature Reviews Cardiology*, vol. 15, no. 2, pp. 97–105, 2018.

[7] R. A. Payne, I. B. Wilkinson, and D. J. Webb, "Arterial Stiffness and Hypertension: Emerging Concepts," *Hypertension*, vol. 55, no. 1, pp. 9–14, 2010.

[8] J. A. Chirinos, P. Segers, T. Hughes, and R. Townsend, "Large-Artery Stiffness in Health and Disease: JACC State-of-the-Art Review," *Journal of the American College of Cardiology*, vol. 74, no. 9, pp. 1237–1263, 2019.

[9] M. E. Safar, B. I. Levy, and H. Struijker-Boudier, "Current Perspectives on Arterial Stiffness and Pulse Pressure in Hypertension and Cardiovascular Diseases," *Circulation*, vol. 107, no. 22, pp. 2864–2869, 2003.

[10] K. Sutton-Tyrrell, S. S. Najjar, R. M. Boudreau, L. Venkitachalam, V. Kupelian, E. M. Simonsick, R. Havlik, E. G. Lakatta, H. Spurgeon, S. Kritchevsky *et al.*, "Elevated Aortic Pulse Wave Velocity, a Marker of Arterial Stiffness, Predicts Cardiovascular Events in Well-Functioning Older Adults," *Circulation*, vol. 111, no. 25, pp. 3384–3390, 2005.

[11] L. M. Van Bortel, S. Laurent, P. Boutouyrie, P. Chowienczyk, J. Cruickshank, T. De Backer, J. Filipovsky, S. Huybrechts, F. U. Mattace-Raso, A. D. Protogerou *et al.*, "Expert consensus document on the measurement of aortic stiffness in daily practice using carotid-femoral pulse wave velocity," *Journal of hypertension*, vol. 30, no. 3, pp. 445–448, 2012.

[12] M. Butlin and A. Qasem, "Large Artery Stiffness Assessment Using SphygmoCor Technology," *Pulse*, vol. 4, no. 4, pp. 180–192, 2017.

[13] V. Fabian, L. Matera, K. Bayerova, J. Havlik, V. Kremen, J. Pudil, P. Sajgalik, and D. Zemanek, "Noninvasive assessment of aortic pulse wave velocity by the brachial occlusion-cuff technique: comparative study," *Sensors*, vol. 19, no. 16, p. 3467, 2019.

[14] T. Shoji, A. Nakagomi, S. Okada, Y. Ohno, and Y. Kobayashi, "Invasive validation of a novel brachial cuff-based oscillometric device (SphygmoCor XCEL) for measuring central blood pressure," *Journal of hypertension*, vol. 35, no. 1, pp. 69–75, 2017.

[15] M. Hwang, J. Yoo, H. Kim, C. Hwang, K. Mackay, O. Hemstreet, W. Nichols, and D. Christou, "Validity and reliability of aortic pulse wave velocity and augmentation index determined by the new cuff-based SphygmoCor Xcel," *Journal of human hypertension*, vol. 28, no. 8, pp. 475–481, 2014.

[16] I. Buraioli, D. Lena, A. Sanginario, D. Leone, G. Mingrone, A. Milan, and D. Demarchi, "A New Noninvasive System for Clinical Pulse Wave Velocity Assessment: The Athos Device," *IEEE Transactions on Biomedical Circuits and Systems*, vol. 15, no. 1, pp. 133–142, 2021.

[17] P. Salvi, G. Lio, C. Labat, E. Ricci, B. Pannier, and A. Benetos, "Validation of a new non-invasive portable tonometer for determining arterial pressure wave and pulse wave velocity: the PulsePen device," *Journal of hypertension*, vol. 22, no. 12, pp. 2285–2293, 2004.

[18] R. Asmar, J. Topouchian, B. Pannier, A. Benetos, M. Safar *et al.*, "Pulse wave velocity as endpoint in large-scale intervention trial. The Complior® study," *Journal of hypertension*, vol. 19, no. 4, pp. 813–818, 2001.

[19] S. S. Hickson, M. Butlin, J. Broad, A. P. Avolio, I. B. Wilkinson, and C. M. McEniery, "Validity and repeatability of the Vicorder apparatus: a comparison with the SphygmoCor device," *Hypertension research*, vol. 32, no. 12, pp. 1079–1085, 2009.

[20] M. Ring, M. J. Eriksson, J. R. Zierath, and K. Caidahl, "Arterial stiffness estimation in healthy subjects: a validation of oscillometric (Arteriograph) and tonometric (SphygmoCor) techniques," *Hypertension Research*, vol. 37, no. 11, pp. 999–1007, 2014.

[21] T. Sondej, I. Jannasz, K. Sieczkowski, A. Dobrowolski, K. Obiała, T. Targowski, and R. Olszewski, "Validation of a new device for photoplethysmographic measurement of multi-site arterial pulse wave velocity," *biocybernetics and biomedical engineering*, vol. 41, no. 4, pp. 1664–1684, 2021.

[22] A. Milan, G. Zocaro, D. Leone, F. Tosello, I. Buraioli, D. Schiavone, and F. Veglio, "Current assessment of pulse wave velocity: comprehensive

review of validation studies," *Journal of hypertension*, vol. 37, no. 8, pp. 1547–1557, 2019.

[23] Y. Ben-Shlomo, M. Spears, C. Boustred, M. May, S. G. Anderson, E. J. Benjamin, P. Boutouyrie, J. Cameron, C.-H. Chen, J. K. Cruickshank *et al.*, "Aortic pulse wave velocity improves cardiovascular event prediction: an individual participant meta-analysis of prospective observational data from 17,635 subjects," *Journal of the American College of Cardiology*, vol. 63, no. 7, pp. 636–646, 2014.

[24] R. A. Rodriguez, V. Cronin, T. Ramsay, D. Zimmerman, M. Ruzicka, and K. D. Burns, "Reproducibility of carotid-femoral pulse wave velocity in end-stage renal disease patients: methodological considerations," *Canadian Journal of Kidney Health and Disease*, vol. 3, p. 109, 2016.

[25] T. Pereira, C. Correia, and J. Cardoso, "Novel Methods for Pulse Wave Velocity Measurement," *Journal of medical and biological engineering*, vol. 35, no. 5, pp. 555–565, 2015.

[26] A. Sanginario, I. Buraioli, M. Boscherini, S. Vitale, C. Sabrina, D. Botto, D. Leone, A. Milan, A. Ciesielski, P. Samorì, and D. Demarchi, "Reduced graphene oxide-based flexible pressure sensor for biomedical applications," *IEEE Sensors Journal*, vol. 24, no. 22, pp. 37 090–37 103, 2024.

[27] A. M. F. V. D. L. F. V. Irene Buraioli, Danilo Demarchi, "Method and system for real-time measurement of the sphygmic wave velocity (pwv)," 2023, uS Patent 18/253,472.

[28] D. Giovanelli, E. Farella *et al.*, "Force Sensing Resistor and Evaluation of Technology for Wearable Body Pressure Sensing," *Journal of Sensors*, vol. 2016, 2016.

[29] A. Sundar, C. Das, and M. Deshmukh, "Novel Applications of Force Sensing Resistors in Healthcare Technologies," in *Proceedings of healthy world conference*, 2015.

[30] C. Lebossé, P. Renaud, B. Bayle, and M. de Mathelin, "Modeling and Evaluation of Low-Cost Force Sensors," *IEEE Transactions on Robotics*, vol. 27, no. 4, pp. 815–822, 2011.

[31] C. Lebossé, B. Bayle, M. de Mathelin, and P. Renaud, "Nonlinear modeling of low cost force sensors," in *2008 IEEE International Conference on Robotics and Automation*. IEEE, 2008, pp. 3437–3442.

[32] A. Valerio, I. Buraioli, A. Sanginario, D. Leone, G. Mingrone, A. Milan, and D. Demarchi, "A new true wireless system for real-time pulse wave velocity assessment," *IEEE Sensors Journal*, 2024.

[33] A. Valerio, I. Buraioli, A. Sanginario, G. Mingrone, D. Leone, A. Milan, and D. Demarchi, "A region-based cross-correlation approach for tonometric carotid–femoral pulse wave velocity assessment," *Biomedical Signal Processing and Control*, vol. 93, p. 106161, 2024.

[34] L. Xu, S. Zhou, L. Wang, Y. Yao, L. Hao, L. Qi, Y. Yao, H. Han, R. Mukkamala, and S. E. Greenwald, "Improving the accuracy and robustness of carotid-femoral pulse wave velocity measurement using a simplified tube-load model," *Scientific reports*, vol. 12, no. 1, p. 5147, 2022.

[35] B. Spronck, D. Terentes-Printzios, A. P. Avolio, P. Boutouyrie, A. Guala, A. Jerončić, S. Laurent, E. C. Barbosa, J. Baulmann, C.-H. Chen *et al.*, "2024 recommendations for validation of noninvasive arterial pulse wave velocity measurement devices," *Hypertension*, vol. 81, no. 1, pp. 183–192, 2024.

[36] F. Asgarian and K. Najafi, "Bluesync: Time synchronization in bluetooth low energy with energy-efficient calculations," *IEEE Internet of Things Journal*, vol. 9, no. 11, pp. 8633–8645, 2021.

[37] T. Sondej and M. Bednarczyk, "Ultra-low-power sensor nodes for real-time synchronous and high-accuracy timing wireless data acquisition," *Sensors*, vol. 24, no. 15, p. 4871, 2024.